Evaluation protocol of skeletonization applied to grayscale curvilinear structures

Rabaa Youssef, Anne Ricordeau, Sylvie Sevestre-Ghalila, Amel Benazza-Benyahya

Evaluation protocol of skeletonization applied to grayscale curvilinear structures

Rabaa Youssef*†, Anne Ricordeau‡, Sylvie Sevestre-Ghalila†, Amel Benazza-Benyahya*
* CEA-LinkLab in Telnet Innovation Labs, Cité Technologique des Communications, Ariana, Tunisia
† COSIM Lab. in Sup'Com., University of Carthage, Cité Technologique des Communications, Ariana, Tunisia
‡ MAP5 Lab. in University of Paris Descartes, UMR CNRS 8145, 45 rue des Saints Pères, Paris, France
rabaa.youssef@supcom.tn, a.ricordeau@iut.univ-paris8.fr, sylvie.ghalila@cea.fr, benazza.amel@supcom.rnu.tn

***Abstract*—Few evaluation protocols were suggested to assess quality of skeletonization methods of grayscale images. Most of these protocols employ criteria and images both devoted to target application. No common image databases are available and the validation of skeleton structural properties under grayscale object variability suffers from a lack of standardized procedures. These properties are namely the preservation of geometry, topology and extremities respectively related to skeleton location and morphological quality. In this paper, we propose an evaluation protocol for skeletonization applied to grayscale curvilinear structures that focuses on skeleton structural properties, regardless of application specificities. We first identify challenging situations for skeletonizing grayscale images and then, construct a synthetic image database of objects with varying contrast, curvature and width. Secondly, we focus on criteria that reflect skeleton structural properties to assess its quality and noise robustness. We apply the proposed protocol on skeletonization methods within differential geometry framework that highlights good skeleton location and morphological thinning category that promotes skeleton connectivity. Experimental results indicate that the proposed protocol is able to describe the behavior of the criteria regarding the structural rendering of skeletonization methods.**

Keywords: grayscale image, skeletonization, evaluation, homotopy, geometry preservation

Introduction

An ideal skeleton has a one-pixel width and is supposed to preserve the geometry and topology (homotopy) of the initial object whereas it should be robust to noise. The first skeletonization methods were proposed in the binary context [1], [2], [3], [4]. They have been applied to grayscale images after a binarization. This preprocessing is questionable as it leads to a loss in information. This drawback has motivated the development of skeletonization methods specially dedicated to grayscale images based either on differential geometry [5], [6] or on mathematical morphology [7], [8]. Each category promotes a prior skeleton property according to target application. In fact, differential methods are interested in good location and smoothness of the crest lines as required in airborne imaging [5], [9], while morphological methods pay more attention to the connectivity of skeletons required in biometric applications [10], in the characterization of bone microarchitecture [11] for biomedical imaging and shape recognition field [12].

Due to the diversity of methods, a need to assess quantitatively skeletonization has arisen. Several evaluation protocols have been proposed for binary methods to validate skeleton structural properties that are homotopy [13], [14], geometry preservation [14], [15], [4], [16], [13] and skeleton robustness to distortions like noise [2], [17], [4] and rotation [17]. On the one hand, these protocols uses either synthetic images of simple curvilinear structures with contour disruptions built by the authors [15], [16], [2], or images from shape recognition databases [14], [18], [17]. Even if authors are standardizing assessment using known image databases, they are constrained to create reference skeletons, unavailable for images from these databases. On the other hand, the reported protocols use evaluation criteria based mainly on good detection rate between reference and resulting skeleton in binary context.

Concerning grayscale skeletonization evaluation, and to the best of our knowledge, very few protocols are available. These protocols concern road extraction application [19], [20] and are namely applied to assess good location and thus, geometry preservation property. The reference skeletons are constructed in this case by experts and the evaluation criteria correspond to statistic indicators of good location of resulting skeleton relatively to the ground truth ones. Consequently, the existing protocols do not validate simultaneously all skeleton structural properties but focus only on application requirements related to geometry preservation while neglecting properties like robustness to noise and preservation of homotopy and extremities. Moreover, no existing grayscale image databases with reference skeletons is available to assess objectively skeleton quality.

In this work, we propose an evaluation protocol for skeletonization devoted to grayscale images with known reference skeletons and using most relevant quality measures in order to assess the skeleton structural properties. The proposed evaluation protocol follows the general scheme proposed by [15] for binary skeletons. It focuses on the design of test images from reference skeletons and on the adequate measure for each skeleton property to be tested. Our contribution consists in objectively assessing

the preservation of geometry, topology and extremities properties under various distortions.
This paper is organized as follows. Section I is devoted to the generation of gray synthetic images reproducing challenging situations for skeletonization of gray curvilinear structures. In Section II, the properties and measures to be used in the assessment are described. Finally, in Section III, the evaluation is conducted on differential geometry based method [5] and two morphological thinning methods [7], [21]. The results are provided and discussed as well as the relevance of the chosen criteria.

I. Synthetic images generation

Since we intend to validate skeleton structural properties that consist in the preservation of geometry, topology and extremities, we need to focus on the challenging grayscale objects configurations that can defy skeletonization. Line crossing, width variation, high curvature, free branches, variable contrast and presence of noise are the main distortions that may affect grayscale curvilinear structures. We propose an automatic procedure for building a database consisting of images that reflect these distortions. To this end, a two-stage procedure is considered. More precisely, we first generate a variety of skeletons from three binary reference skeletons presenting structural specificities: lines with high curvature, intersections and free branches. Secondly, by using mathematical morphological and filtering tools, we generate distorted versions of images containing these skeletons with various topographic reliefs.
The first objective is to design images to validate the detection of closed lines with high curvature. In this respect, we choose an initial binary image containing a reference skeleton S_{R} representing a ring (without end) wich contains two concentric circular skeletons $S^*_{R_1}$ and $S^*_{R_2}$ with respectively radii R_1 and R_2 ($R_1 < R_2$). To $S^*_{R_1}$ (resp. $S^*_{R_2}$), we apply a dilation δ_{ρ_1} (resp. δ_{ρ_2}) with a ball as structuring element of radius ρ_1 (resp. ρ_2). Then, we average the image using a convolution circular kernel f_{r_f} of radius size r_f. In the resulting smooth image, the average difference D between the object level and the background is used to quantify the contrast variation between the object and the background. We can adjust this contrast at will by multiplying the gray levels by a factor $C \in [0, 1]$. Finally, a Gaussian noise n_σ of variance σ^2 is added to obtain the synthetic noisy image I_R:

$$I_{\mathrm{R}} = C\left(\left[\delta_{\rho_1}(S^*_{R_1}) + \delta_{\rho_1}(S^*_{R_2})\right] * f_{r_f}\right) + n_\sigma. \qquad (1)$$

The leftmost column in Figure 1 illustrates the generation of the test images with $R_1 = 74$ and $R_2 = 145$. The employed dilations correspond to binary disks of respectively radii $\rho_1 = 4$ and $\rho_2 = 9$ and the size of the kernel is $r_f = 9$. A high contrast in I_{R} is achieved thanks to a multiplicative factor $C = 0.8$ which allows us to have $D = 81$ (gray levels within $[0, 255]$).
Similarly, we generate the network image I_{N} of Figure 1 from the reference skeleton S^*_{N}. We use this image to test the ability of skeletonization methods to preserve connectivity and free extremities and to detect low-contrast lines ($D = 46$). The gray network is obtained after a binary dilation with a disk of radius $\rho = 1$ followed by an averaging with a filter of kernel radius $r_f = 7$.
To study the ability of the skeletonization to detect interconnected lines even if their widths vary, we construct an image $I_\cap$ displayed in Figure 1 which is a simple intersection of lines with different widths.
For all the generated images, we use a uniform background gray level (set to 25 in Figure 1) to avoid any truncation of the added noise values on the original images when simulating distortions.

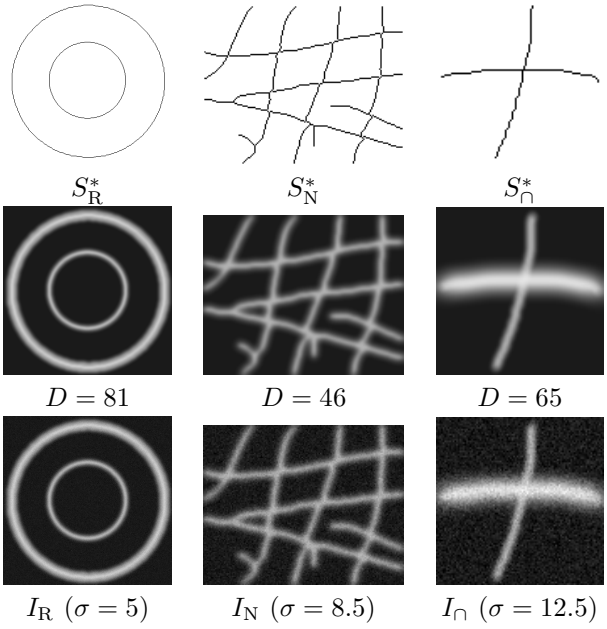

Fig. 1. First line: binary reference skeletons S^*_{R}, S^*_{N} and S^*_{I}. Second line: smooth gray images with an average contrast D between foreground and background. Third line: Image affected by an additive Gaussian noise on the gray images of second line with I_{R}: 326×326, I_{N}: 150×121, $I_\cap$: 100×100.

II. Evaluation criteria and measures

A. Review of existing criteria and measures

Table I summarizes the criteria and measures reported in the literature to assess skeleton properties. The two most important ones are skeleton morphological and location quality.
For the first criterion, Hausdorff and Dubuisson distances are frequently used to assess geometry preservation property under noise degradation and image rotation [2], [17]. However, these distances do not reflect the type of dissimilarity between the modified skeleton S and the reference one S^*. For instance, they do not provide any information about missing or extra branches. Other authors used the *Area* operator which consists in counting skeleton pixels

TABLE I
BINARY SKELETONIZATION EVALUATION: FROM SKELETON PROPERTY TO APPLIED MEASURES.

	Skeleton property	Name of skeleton quality	Associated measures
Structural properties	Preservation of geometry	Location quality: Similarity to medial axis	Counting pixels (*Area* operator): [22]
			No explicit formula: [15]
			Counting pixels (*Area*): [4]
			Ratio based on euclidian distance between real and reference skeleton pixels: [14]
			Hausdorff distance: [16], [2]
			Hausdorff & Dubuisson distances: [17]
			Qualitative (observation) [18]
	Preservation of topology and extremities	Mophological quality	Number of branches and nodes: [14]
			Number of connected components: [13]
			Number of spurious branches based on orientation + length inferior to object half-width [13]
	Reconstruction		Counting pixels (*Area*): [14]
	Unitary thickness		Counting pixels (*Area*): [4]
	Computational speed	Computation time	Mean computation time for all database characters for each method: [14]

and calculating ratio between S and S^* [22], [4], [16], [13]. This operator is also involved in the *buffer width* measure based on statistical indicators of true/false detection. The buffer width method is particularly widespread for assessing road detection methods [20]. Its advantage is the use of indicators that enable to interpret possible dissimilarity between S and S^* using a buffer zone.

Concerning homotopy, few protocols have investigated this property. A counting of connected components and extremities are the main employed measures to describe the skeleton ability to preserve connectivity and manage spurious branches.

In conclusion to this review of properties, we note that statistical indicators of *buffer width* are relevant for geometry preservation property since they enable us to interpret the skeleton quality regarding the deviation of branches in S compared to S^*. A straightforward way to evaluate objectively skeleton morphological quality (homotopy and extremity preservation) is a counting of its connected components and extremities [14], [13].

B. Buffer method for geometry preservation property

The benefit of using the *buffer method* is mainly related to its indicators based on statistic indicators of good/bad detection. First, a dilation using disk structuring element of radius ρ is applied to the reference S^* or the extracted skeleton S to calculate respectively the matched extraction or matched reference with tolerated displacement. Second, the three indicators are calculated: (TP) which is the number of successfully matched extraction, (FP) as the number of wrongly extracted skeleton pixels and (FN) which corresponds to the number of missing reference in the detection. These ratios are illustrated in Figure 2 for a simple straight line and calculated according to the following formula:

$$TP = S \cap \delta_\rho(S^*), \quad FP = S \cap \overline{\delta_\rho(S^*)}, \quad FN = S^* \cap \delta_\rho(S).$$

Finally, the completeness Cp and correctness Cr measures are defined to evaluate the geometrical accuracy of the real skeleton compared to the reference one:

$$Cp = TP/(TP + FN), \quad Cr = TP/(TP + FP).$$

In order to get meaningful values of Cp and Cr, the radius

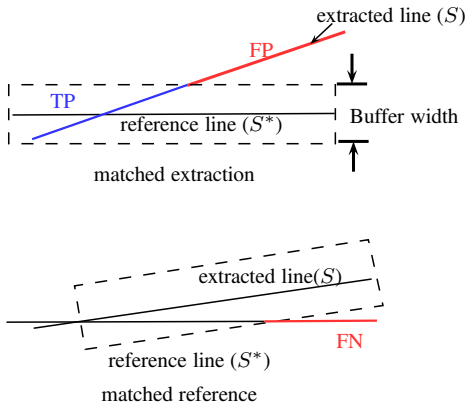

Fig. 2. Matched reference and extraction for the buffer method on a simple straight line skeleton [20].

ρ of the structuring element should not be greater than half-width of the curvilinear structures. Consequently, we choose for each image the smallest radius ρ of binary dilation according to the synthetic images generation process if more than one disk was used. Therefore, for the network image I_{N}, *buffer* width corresponds to $\rho = 1$, while $\rho = 5$ for the rings image I_{R} and $\rho = 3$ for the intersection $I_{\cap}$.

An example of the *buffer method* operating is given in Figure 3 and shows the results of the Cp and Cr calculation. In this example, we illustrate true positive TP, false negative FN and false positive FP measures. When the obtained skeleton is shortened by the skeletonization method, this affects the completeness Cp indicator, while apparition of extra branches or a significant deviation from the reference induces a decrease of Cr.

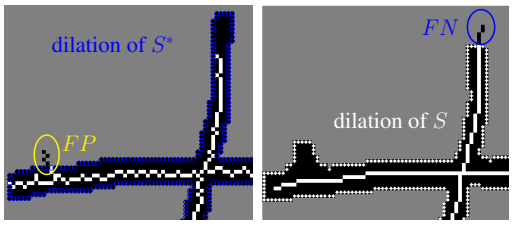

(a): $Cr = 97.29\%$ (b): $Cp = 97.81\%$

Fig. 3. Operating *buffer method* for the calculus of Cp and Cr.

C. Counting endpoints, connected components of the background and foreground for homotopy property

By definition, homotopy preserves the background and foreground connectivity. Therefore, counting the number of connected components for both background and foreground is a direct measure of this property. We add to this measure the number of skeleton ends to identify spurious branches rarely considered in the existing evaluation protocols [13]. At the first glance, the emergence of spurious branches could be reflected by Cr. However, spurious branches small lengths often hide them when dilating the reference skeleton to calculate FP and then Cr indicator. Since the complementary connectivity between the background and the object must be selected to meet the requirement of Jordan theorem, we choose 8-connectivity for the foreground (object) and 4-connectivity for the background when counting their respective number of connected components. The homotopy is objectively measured by the following normalized differences BCC, OCC and E:

$$BCC = \frac{\text{Nb BCC}(S^*) - \text{Nb BCC}(S)}{\text{Nb BCC}(S^*)},$$

$$OCC = \frac{\text{Nb OCC}(S^*) - \text{Nb OCC}(S)}{\text{Nb OCC}(S^*)},$$

$$E = \frac{\text{Nb E}(S^*) - \text{Nb E}(S)}{\text{Nb E}(S^*)}$$

where Nb BCC denotes the number of background components, Nb OCC is the number of object components and, Nb E is number of skeleton ends. The ideal values for BCC, OCC and E are around zero, negative ratios correspond to the emergence of extra and insignificant information while positive values correspond to missing information in the real skeleton. These measures may diverge, as in the case where the number of ends of S is much larger than that of S^*. Hence, large values (respectively small) are clipped to 5 (respectively -5).
These measures can be combined in a single performance score integrating the different quality measures for the assessment of skeletonization as proposed by [13]. For instance, the global performance score could be a weighted average of BCC, OCC and E, the weights being adjusted according to their importance for the target application.

III. Implementation of the evaluation protocol

A. Choice of tested skeletonization methods

We have retained the most representative and known methods of the class of differential skeletonization and the class of morphological thinning for which source codes are available. The Differential Line Detector (DLD) [5] is a representative method of the first class. It results from a sub-pixel skeleton and is applied particularly to satellite images for the detection of roads. The λ-Skeleton of [7] implemented in Pink library and Statistically Controlled Thinning (SCCT) of [21] represent the retained methods of the second category. These thinning methods focus on the connectivity of skeleton, while DLD is interested in the good detection of ribbon-like structures. We detail in Table II the required parameters setting of each method and indicate how dependent they are on user intervention. We note according to Table II that DLD requires three

TABLE II
Parameters setting for the skeletonization methods.

Method	Parameters	Setting
DLD	Gaussian kernel standard deviation	$\sigma_{\text{DLD}} \sim \sqrt{3}.w$ with w object line width
	Hysteresis thresholds:	$high = f(w,h)$ with h image contrast
		$low \in [0.2high, 0.5high]$
Pink	Contrast parameter	λ: manually set
SCCT	Test significance level	$\alpha \in [10^{-6}, 10^{-2}]$
	Noise standard deviation	σ

parameters to be set, the first is related to the half-width w of object lines and therefore selects the range of lines to be detected by the method. The other two parameters are hysteresis thresholds also dependent on w and on image contrast h. The SCCT implementation takes two parameters. The first is related to noise standard deviation of the image, and the second the test significance level α. The λ-Skeleton of Pink library admits a unique global parameter manually set which allows to filter non significant skeleton information. We evaluate the λ-Skeleton performance using two options: eliminating all peaks and ends (Pink1) or maintaining extremities (Pink2).

B. Results

A set of $N = 60$ synthetic images is produced by varying the standard-deviation σ of the additive white Gaussian noise n_σ within $[2.5, 12.5]$ by a step of 0.5. From these images, the skeletons are extracted with the three retained methods. Some of the resulting skeletons are displayed in Figure 4 whereas the average measures of Cp, Cr, OCC, BCC and E are presented in Table III. We suggest to evaluate the global performance of the skeletonization methods by using the following global score P:

$$P = 1 - [((1-Cp) + (1-Cr) + (OCC^*) + (BCC^*) + E^*]/5$$

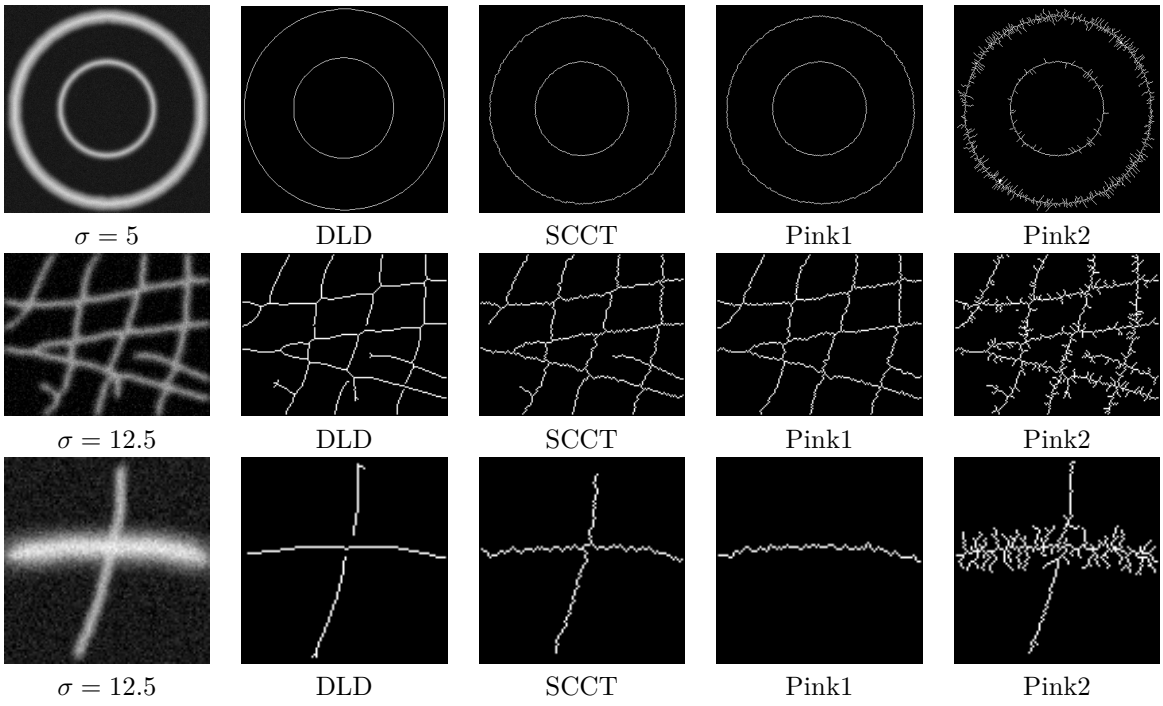

Fig. 4. Skeletonization methods results on I_{R}, I_{N} and $I_{\cap}$.

where OCC^*, BCC^* and E^* are the normalized versions (in $[0, 1]$) of the indicators. This score is an average value of Cp, Cr, OCC, BCC and E measured for each method. We choose to calculate this global score using the average values of each indicator for the three images and the considered noise levels. Table III summarizes the mean indicators of Cp, Cr, OCC, BCC and E and the corresponding score P. We first discuss the results according to geometry preservation criteria. The measures of Cp, Cr in Table III are maximal for DLD. In fact, as illustrated in Figure 4, the DLD skeleton is smooth for the 3 images and its quality is not affected neither by contrast changes, additive noise nor high curvature. Skeleton lines are correctly positioned on center lines and this is due to the smoothing step performed before the crest points detection process. For Pink library implementation of the λ-Skeleton, we note lower performance of the method (for both options Pink1 and Pink2) compared to SCCT. In fact, the first option (removing all ends and peaks) impacts the completeness Cp of the skeleton. The second option affects the correctness Cr of the skeleton since spurious branches are detected. Secondly, we focus on skeleton morphological quality linked to homotopy preservation (OCC, BCC, E). According to these indicators, SCCT appears to meet a tradeoff between correctly detecting the connected components of the background/foreground, and preserving the significant extremities. On the one hand, DLD indicators for object and background connectivity are the less accurate compared to Pink1 results and to SCCT ones. This is explained by the fact that differential methods do not put constraints on homotopy and assume that all the object lines have similar widths. On the other hand, results based on Pink2 diverges from the expected results concerning the extremities preservation measure E. We find out that the SCCT method is stable according to both geometry and homotopy indicators. If the global evaluation score P is decomposed, we notice that for SCCT, the average spatial positioning is correct, the homotopy indicators are close to zero whereas Pink and DLD. This method results are less impacted by disruptions, high curvatures, changing line widths, contrast and free extremities.

We may conclude according to the evaluation results that completeness Cp and correctness Cr initially introduced to assess geometry preservation property (skeleton positioning quality) provide also information on the persistence of spurious branches that affect particularly thinning methodologies. In addition, topological definitions of connected components and skeleton extremities make the calculus of connectivity rates BCC, OCC and E straightforward and thus, ensure a relevant evaluation of skeleton morphological quality.

TABLE III
AVERAGE INDICATORS VALUES FOR EACH METHOD.

Methods	Cp	Cr	OCC	BCC	E	P
DLD	1.00	1.00	-1.81	0.11	-0.15	0.92
SCCT	0.97	0.98	0.01	0.03	0.17	0.98
Pink1	0.86	1.00	0	0	0.19	0.96
Pink2	1.00	0.81	-3.89	0.003	-5.00	0.61

Conclusion

A review of evaluation protocols of skeletonization methods led us to conclude that the assessment of gray skeletonization methods has been little addressed in existing works. Inspired by existing binary protocols, we design a new one focusing on methods applied to grayscale images and assessing skeleton qualities. We propose to conduct the evaluation according to objective indicators that can reflect structural properties of skeletonization: preservation of geometry, topology and extremities.

We generate synthetic grayscale images database including real images distortions to test one at a time, the ability of skeletonization methods to adapt to low/high contrast, high curvature, presence of free branches, line crossings and varying widths and noise since we noticed a dependency of the methods setting to these distortions.

According to evaluation results, we may conclude on the quality of the relevant chosen measures to validate skeleton structural properties. It is worth noting that the evaluation protocol scheme adopted in this work is applicable to binary images under the unique constraint of considering binary images and corresponding distortions.

The relevance of the skeleton quality measures used in the proposed evaluation protocol enables to conclude to the applicability of studied skeletonization methods in certain fields of application. In fact, the importance of specific skeleton properties may be discussed depending on the area of applications. If a smooth skeleton is required with no real need to preserve connectivity (images with no intersections), the differential methods are well adapted to such applications. This explains the interest given to this category of methods in the field of road detection. On the other hand, for applications like biometric matching process or trabecular bone structure characterization, the skeleton connectivity is a first priority since it is employed to compute features such as number of nodes, extremities and segments. Therefore, thinning approaches are well adapted to such contexts.

The proposed evaluation protocol can be used to adjust and interpret the required parameters for the tested methods. Indeed, we note that the manual setting of λ-Skeleton parameter is intimately linked to the intensity of noise on images, while the α parameter of SCCT or h of DLD depends on the contrast.

References

[1] H. Blum, "A transformation for extracting new descriptors of shape," in *Proc. on Models for the Perception of Speech and Visual Form*, W. Wathen-Dunn, Ed. Cambridge, MA: MIT Press, November 1967, pp. 362–380.

[2] T. Grigorishin, G. H. Abdel-Hamid, and Y. H. Yang, "Skeletonisation: An electrostatic field-based approach," *Pattern Analysis and Applications*, vol. 1, no. 3, pp. 163–177, 1998.

[3] L. Lam, S. W. Lee, and C. Y. Suen, "Thinning methodologies - a comprehensive survey," *IEEE Transactions on Pattern Analysis and Machine Intelligence*, vol. 14, no. 9, pp. 869–885, 1992.

[4] B. K. Jang and R. T. Chin, "One-pass parallel thinning: analysis, properties, and quantitative evaluation," *IEEE Transactions on Pattern Analysis and Machine Intelligence*, vol. 14, no. 11, pp. 1129–1140, 1992.

[5] C. Steger, "An unbiased detector of curvilinear structures," *IEEE Transactions on Pattern Analysis and Machine Intelligence*, vol. 20, no. 2, pp. 113–125, 1998.

[6] G. Lisini, C. Tison, F. Tupin, and P. Gamba, "Feature fusion to improve road network extraction in high-resolution sar images," *IEEE Geoscience and Remote Sensing Letters*, vol. 3, no. 2, pp. 217–221, 2006.

[7] M. Couprie, F. N. Bezerra, and G. Bertrand, "Grayscale image processing using topological operators," in *Proc. of SPIE Vision Geometry VIII.*, vol. 3811, September 1999, pp. 261–272.

[8] C. Arcelli and L. Serino, "Skeletonization of labeled gray-tone images," *Image and Vision Computing*, vol. 23, no. 2, pp. 159 – 166, 2005.

[9] H. Chu, L. Zi-xian, Y. Fang, D. Xin-ping, and L. Ming-sheng, "Road extraction from sar imagery based on multiscale geometric analysis of detector responses," *Selected Topics in Applied Earth Observations and Remote Sensing, IEEE Journal of*, vol. 5, no. 5, pp. 1373–1382, Oct 2012.

[10] J. A. Unar, W. C. Seng, and A. Abbasi, "A review of biometric technology along with trends and prospects," *Pattern Recognition*, vol. 47, no. 8, pp. 2673 – 2688, 2014.

[11] S. Sevestre-Ghalila, A. Benazza-Benyahia, A. Ricordeau, N. Mellouli, C. Chappard, and C. L. Benhamou, "Texture image analysis for osteoporosis detection with morphological tools," in *Medical Image Computing and Computer-Assisted Intervention*, ser. Lecture Notes in Computer Science, C. Barillot, D. Haynor, and P. Hellier, Eds. Springer Berlin Heidelberg, 2004, vol. 3216, pp. 87–94.

[12] S. Wshah, Z. Shi, and V. Govindaraju, "Segmentation of arabic handwriting based on both contour and skeleton segmentation," in *IEEE Proc. Int. Conf. on Document Analysis and Recognition*, 2009, pp. 793–797.

[13] A. Al-Shatnawi, K. Omar, B. AlFawwaz, and A. Zeki, "Skeleton extraction: Comparison of five methods on the arabic ifn/enit database," in *Proc. Int. Conf. on Computer Science and Information Technology*, March 2014, pp. 50–59.

[14] S. Lee, L. Lam, and C. Suen, "Performance evaluation of skeletonization algorithms for document analysis processing," in *Proc. Int. Conf. on Document Analysis and Recognition*, 1991, pp. 260–271.

[15] R. M. Haralick, "Performance characterization in image analysis: thinning, a case in point," *Pattern Recognition Letters*, vol. 13, no. 1, pp. 5 – 12, 1992.

[16] M. Y. Jaisimha, R. M. Haralick, and D. Dori, "A methodology for the characterization of the performance of thinning algorithms," in *Proc. Int. Conf. on Document Analysis and Recognition*, October 1993, pp. 282–286.

[17] J. Chaussard, M. Couprie, and H. Talbot, "Robust skeletonization using the discrete λ-medial axis," *Pattern Recognition Letters*, vol. 32, no. 9, pp. 1384–1394, 2011.

[18] X. Bai, L. J. Latecki, and W. Y. Liu, "Skeleton pruning by contour partitioning with discrete curve evolution," *IEEE Transactions on Pattern Analysis and Machine Intelligence*, vol. 29, no. 3, pp. 449–462, Mar. 2007.

[19] C. Heipke, H. Mayer, C. Wiedemann, and O. Jamet, "Evaluation of automatic road extraction," in *Int. Archives of Photogrammetry and Remote Sensing*, 1997, pp. 47–56.

[20] G. Xufeng, D. Dean, S. Denman, C. Fookes, and S. Sridharan, "Evaluating automatic road detection across a large aerial imagery collection," in *Proc. Int. Conf. on Digital Image Computing Techniques and Applications*, Dec 2011, pp. 140–145.

[21] R. Youssef, S. Sevestre-Ghalila, and A. Ricordeau, "Statistical control of thinning algorithm with implementation based on hierarchical queues," in *IEEE Proc. Int. Conf. on Soft Computing and Pattern Recognition*, Aug 2014, pp. 365–370.

[22] B. Jang and R. Chin, "Analysis of thinning algorithms using mathematical morphology," *IEEE Transactions on Pattern Analysis and Machine Intelligence*, vol. 12, no. 6, pp. 541–551, 1990.